Ibn Al-Haitham Journal for Pure and Applied Sciences
Journal homepage: jih.uobaghdad.edu.iq

Rotation and Magnetic Force Effects on Peristaltic Transport of Non -Newtonian Fluid in a Symmetric Channel

Amaal Mohi Nassief
Department of Mathematics, College of Science, University of Baghdad, Baghdad, Iraq
laama82@yahoo.com

Ahmed M. Abdulhadi
Department of Mathematics, College of Science, University of Baghdad, Baghdad, Iraq
ahm6161@yahoo.com

Article history: Received 1 October 2022, Accepted 12 December 2022, Published in April 2023.

doi.org/10.30526/36.2.3066

Abstract

In this paper, the impact of magnetic force, rotation, and nonlinear heat radiation on the peristaltic flow of a hybrid bio -nanofluids through a symmetric channel are investigated. Under the assumption of a low Reynolds number and a long wavelength, the exact solution of the expression for stream function, velocity, heat transfer coefficient, induced magnetic field, magnetic force, and temperature are obtained by using the Adomian decomposition method. The findings show that the magnetic force contours improve when the magnitude of the Hartmann number M is high and decreases when rotation increases. Lastly, the effects of essential parameters that appear in the problem are analyzed through a graph. Plotting all figures is done using the MATHEMATICA software.

Keywords Adomain decomposition technique, Peristaltic transport, Magnetic force, Symmetric channel, Rotation frame.

1. Introduction

Recently, nanotechnology has gained a lot of attention. The performance of this field in several applications, such as photocatalysts, heat exchangers, engineering, and biomedicine such as destroying tumor cells and cancer diagnosis was studied in the modern era. Many nanoparticles such as copper, gold, and silver particles are used in proteins and nucleic acids. Because these nanoparticles have highly biocompatible, magnetic, chemical, mechanical, and thermal properties. Due to their superior quenching efficiency when compared to other nanoparticles, nanoparticles are widely used in medicinal applications for the treatment of malignant tumors[1-3].

Peristaltic is a significant mechanism produced by the propagation of waves all along the walls of a tube or a channel. This mechanism is well known to physiologists as one of the principle mechanisms for fluid transportation. Peristaltic mechanisms are utilized in a variety of industrial applications and biomedical, this mechanism is helpful in many different systems, including the motion of ovulation in the fallopian channel, the swallowing of food down to the stomach, the flow

of tiny blood vessels, blood pump in the heart-lung machine, and the transport of urine from the renal to the bladder[4]. There are some academic research has investigated the peristaltic flow process of nanofluids, and some of these researches, including . [5] discussed the peristaltic transport affects the magnetic field and thermal properties of copper-water nanofluids. [6] discussed Zinc Oxide nanoparticles moving via tapering arteries while suspended in blood and subject to magnetic effects. [7] examined the impacts of various nanoparticle types on the peristaltic transport of nanofluid. [8] studied the impact of the apply magnetic field on heat radiation and the magnetic force on gold and copper nanoparticles in peristaltic flow. [9] discussed the effect of nanoparticles in the motion of blood in a vertical channel. [10] discussed the peristaltic of couple stress nanofluid organized by the presence the electrical field and magnetic field into micro channel.

The rotation phenomenon has several uses in cosmic and geophysical processes .It can be used to understand when galaxies arise and the oceans circulate. The orientation of nanoparticles in fluids is explained by rotational diffusion.The peristalsis of magnetic field fluid in the presence of rotation is significant in some flow situations involving the motion of physiological fluids, such as saline water and blood. The magnetic field and rotation are beneficial for the movement of bio fluids through the intestines, ureters, and arterioles. Numerous scholars have been interested in the impact of rotation and the peristaltic transport mechanism since they were examined by [11-17].

This study intends to investigate how both magnetic force and rotation affect the peristaltic transport of hybrid bio-nanofluids through a symmetric channel. The precise solutions for magnetic force, stream lines, heat transfer coefficient, temperature, and velocity have been obtained utilizing the Adomian decomposition technique. Graphs are used to illustrate physical characteristics that affect the flow.

2. Adomain Decomposition Method (ADM)

This method can be utilized to solve linear and non-linear differential equations as well as integral equations, and it produces better results than other methods. George Adomian first proposed this method, and it has since been used to solve a variety of problems[18 and19]. To illustrate a general overview of the Adomain Decomposition Method, let's consider a form equation [20-23].

$$Lu + Ru + Nu = g \tag{1}$$

Where L is invertible linear operator, N represent the nonlinear terms, R is reminder of the linear operator. Applying the L^{-1} on both sides in equation (1), yield:

$$u = \mathrm{L}^{-1}(g) - \mathrm{L}^{-1}(Ru) - \mathrm{L}^{-1}(Nu) \tag{2}$$

Now L^{-1} represent the n-fold integration for nth order L,by using the given conditions all are assumed to be prescribed ,the ADM define the solution:

$u = \sum_{m=0}^{\infty} u_m$.

Where the $u_0, u_1, u_3, \ldots$ recursively determined by using the relation :

$u_0 = f(x)$,

$$u_{m+1} = \mathrm{L}^{-1}(R\ u_m) - \mathrm{L}^{-1}(N\ u_m)\,, m \geq 0 \qquad (3)$$

The last term of the Eq. (3) can be computed by substituting :

$$Nu = \sum_{m=0}^{\infty} A_m(u_0\,, u_1, \ldots, u_m)\,.$$

Where A_m represent generated Adomain polynomials for the specified nonlinearity, they depend only on the $u_0\,, \ldots, u_m$ components and form rapidly converge series, the A_m are given:

$A_0 = f(u_0)$,

$A_1 = u_1 f^{(1)}(u_0)$,

$A_2 = u_2 f^{(1)}(u_0) + \frac{u_1^2}{2!} f^{(2)}(u_0)$.

And can be found from the formula :

$$A_m = \frac{1}{m!}\frac{d^m}{d\lambda^m}\left[N\left(\sum_{i=0}^{\infty}\lambda^i u_i\right)\right]_{\lambda=0}\,.$$

3. Problem Formulation

Let's consider the peristaltic flow of an electrically conducted hybrid bio-nanofluid in the presence of rotation and magnetic field, blood is considered in this research as a basic non-Newtonian fluid, while copper and gold are considered nanoparticles in a 2-D channel of width $2d_1$. A $(\overline{\mathrm{X}}, \overline{\mathrm{Y}})$ Cartesian coordinate system. We selected $\overline{\mathrm{X}}$ in the direction of wave propagation and $\overline{\mathrm{Y}}$ transverse to it, a constant magnetic field of strength H_0 acting in the transverse direction results in an induced magnetic field $H\big(\overline{H}_x(\overline{\mathrm{X}}, \overline{\mathrm{Y}}, \bar{\mathrm{t}}), \overline{H}_y(\overline{\mathrm{X}}, \overline{\mathrm{Y}}, \bar{\mathrm{t}}) + H_0, 0\big)$. H*refers to the total magnetic field composed of $\big(\overline{H}_x(\overline{\mathrm{X}}, \overline{\mathrm{Y}}, \bar{\mathrm{t}}), \overline{H}_y(\overline{\mathrm{X}}, \overline{\mathrm{Y}}, \bar{\mathrm{t}}) + H_0, 0\big)$. The channel wall's geometry is depicted by:

$$h = \xi(\overline{\mathrm{X}}, \bar{\mathrm{t}}) = d_1 + d_2\, Sin\left(\frac{2\pi}{\lambda}(\overline{\mathrm{X}} - \mathrm{C}\bar{\mathrm{t}})\right) \qquad (4)$$

The flow of the fluid is induced by the infinite sinusoidal wave that travels along the channel walls at a wave speed of C and a wavelength of λ. Where d_2 is the wave amplitude, d_1 is the half channel width, and $\bar{\mathrm{t}}$ is the time. The governing for the problem are:

$$\nabla . E = 0 \quad , J = \nabla \times H\,,\ \nabla . H = 0\,,\ \ \sigma[E + \mu_e(V \times H^*)] = J,$$

$$\nabla \times E = -\mu_e \frac{\partial H}{\partial t} \qquad (5)$$

Where **V** is velocity vector, **σ** is electrical conductivity**, J** is current density; **E** is electric field ,and $\boldsymbol{\mu_e}$ is magnetic permeability. The governing equations for an incompressible, unsteady, hydro-magnetic, viscous bio- nanofluid (Au-Cu Nanoparticles) include momentum, induction, and heat [24and 25]:

$$\nabla . V = 0 \tag{6}$$

$$\rho_{nf}\frac{\partial V}{\partial t} + \rho_{nf}(\bar{\Omega} \times (\bar{\Omega} \times V) + 2\bar{\Omega} \times \frac{\partial V}{\partial t} = -\nabla P + \mu_{nf}\nabla^2 V + \mu_e(H^* . \nabla)H^* - \mu_e\frac{\nabla H^{*2}}{2} \tag{7}$$

$$\frac{\partial H^*}{\partial t} = \nabla \times (V \times H^*) + \frac{1}{\zeta}\nabla^2 H^* \tag{8}$$

$$(\rho c_p)_{nf}\frac{DT}{Dt} = k_{nf}\nabla^2 T + \mu_{nf}(\nabla V + (\nabla V)^T)^2 - \frac{\partial q}{\partial Y} + Q_0 \tag{9}$$

Where P is fluid pressure, $\zeta = \mu_e\sigma_{nf}$, represent the magntic diffusivity, σ_{nf} is the electrical conductivity,T represent the temperature distribution, $q = -\frac{4\sigma_f^*}{3k_f^*}\frac{\partial T^4}{\partial Y}$ is the radiative heat flux, k_f^* and σ_f^* are mean absorption coeffient and Stefan Boltzmann constants, Q_0 is the heat source, experimental formulation for the physical characteristics of hybrid nanofluid[25] are shown in Table 1, which are given by:

Table 1 Physical properties of hybrid nanofluid **.**

property	**Nanofluids**
Density	$\rho_{nf} = \left((1-\emptyset_1)\rho_f + \emptyset_1\rho_1\right)(1-\emptyset_2) + \emptyset_2\rho_2$
Heat capacity	$(\rho c_p)_{nf} = \left((\rho c_p)_f(1-\emptyset_1) + (\rho c_p)_1\emptyset_1\right)(1-\emptyset_2) + (\rho c_p)_2\emptyset_2$
Dynamic viscosity	$\mu_{nf} = \frac{\mu_f}{(1-\emptyset_1)^{2.5}(1-\emptyset_2)^{2.5}}$
Thermal conductivity	$k_{nf} = \left(\frac{k_2 + (m-1)k_3 - (k_3-k_2)\emptyset_2(m-1)}{k_3(m-1) + k_2 + \emptyset_2(k_3-k_2)}\right)k_3$
	$k_3 = \left(\frac{k_1 + k_f(m-1) - (k_f-k_1)(m-1)\emptyset_1}{k_1 + \emptyset_1(k_f-k_1) + k_f(m-1)}\right)k_f$
Ectrical conductivity	$\sigma_{nf} = \sigma_3\left(\frac{\sigma_2(1+2\emptyset_2) + 2(1-\emptyset_2)\sigma_3}{\sigma_3(2+\emptyset_2) + \sigma_2(1-\emptyset_2)}\right)$ $\sigma_3 = \sigma_f\left(\frac{\sigma_1(1+2\emptyset_1) + 2\sigma_f(1-\emptyset_1)}{\sigma_1(1-\emptyset_1) + \sigma_f(2+\emptyset_1)}\right)$

Where $\emptyset_1$ is the volume fraction of gold nanoparticles, $\emptyset_2$ is the volume fraction of copper nanoparticles, and m represents the shape of a factor of the indicated nanoparticles, respectively. The physical characteristics of nanoparticles are classified in the **Table 2**.

Table 2. Based fluid and nanoparticles properties[25].

Properties	**Based fluid**	**Nanoparticle (Gold Au)**	**Nanoparticle (Copper Cu)**
ρ density	$\rho_f = 1050$	$\rho_1 = 19300$	$\rho_2 = 8933$
C_p heat capcity	$C_{pf} = 3617$	$C_{p1} = 129$	$C_{p2} = 385$
K thermal conductivity	k_f=0.52	$k_1 = 318$	$k_2 = 401$
σ electrical conductivity	$\sigma_f = 1.33$	$\sigma_1 = 4.1 * (10^7)$	$\sigma_2 = 5.96 * (10^7)$

The velocity $\vec{\mathbf{V}}$ of 2-D flows $\overrightarrow{\mathbf{V}}$ is defined as $[\bar{U}(\bar{X},\bar{Y},\bar{t}),\bar{V}(\bar{X},\bar{Y},t),0]$, where $\bar{U}$ denotes the velocity component in coordinate $\bar{X}$ and $\bar{V}$ denotes the velocity component in coordinate $\bar{Y}$.

Choose a wave frame$(\overline{x},\bar{y})$ that moves at a speed of C away from the fixed frame by the following transformation given below.

$$\bar{x} = \bar{X} - C\bar{t}, \quad \bar{Y} = \bar{y} \ , \bar{u} = \bar{U} - C \ , \bar{V} = \bar{v} \tag{10}$$

The governing equations were simplified to take the following form:

$$\frac{\partial \bar{u}}{\partial \bar{x}} + \frac{\partial \bar{v}}{\partial \bar{y}} = 0 \tag{11}$$

$$\rho_{nf}\left(\bar{u}\frac{\partial \bar{u}}{\partial \bar{x}} + \bar{v}\frac{\partial \bar{u}}{\partial \bar{y}}\right) - \rho_{nf}\Omega\left(\Omega(\bar{u}) + 2\frac{\partial \bar{v}}{\partial \bar{t}}\right) = -\frac{\partial \bar{p}}{\partial \bar{x}} + \mu_{nf}\left(\frac{\partial^2}{\partial \bar{x}^2} + \frac{\partial^2}{\partial \bar{y}^2}\right)\bar{u} - \frac{\mu_e}{2}\frac{\partial \bar{H}^{*2}}{\partial \bar{x}} + \mu_e \left(\bar{H}_x\frac{\partial\, \bar{H}_x}{\partial \bar{x}} + \quad (\bar{H}_y + H_0)\frac{\partial\, \bar{H}_x}{\partial \bar{y}}\right) \tag{12}$$

$$\rho_{nf}\left(\bar{u}\frac{\partial v}{\partial \bar{x}} + \bar{v}\frac{\partial \bar{v}}{\partial \bar{y}}\right) - \rho_{nf}\Omega\left(\Omega\bar{v} + 2\frac{\partial \bar{u}}{\partial \bar{t}}\right) = -\frac{\partial \bar{p}}{\partial \bar{y}} + \mu_{nf}\left(\frac{\partial^2}{\partial \bar{x}^2} + \frac{\partial^2}{\partial \bar{y}^2}\right)\bar{v} - \frac{\mu_e}{2}\frac{\partial \bar{H}^{*2}}{\partial \bar{y}} + \mu_e \left(\bar{H}_x\frac{\partial\, \bar{H}_y}{\partial \bar{x}} + (\bar{H}_y + H_0)\frac{\partial}{\partial \bar{y}}\bar{H}_y\right) \tag{13}$$

$$\frac{1}{\mu_e}\frac{\partial \bar{E}}{\partial \bar{y}} = \frac{\partial \bar{u}}{\partial \bar{y}}\left(\bar{H}_y + H_0\right) - \frac{\partial \bar{v}}{\partial \bar{y}}\bar{H}_x + \frac{1}{\zeta}\nabla^2 H_x^* \tag{14}$$

$$(\rho c_p)_{nf}\left(\bar{u}\frac{\partial}{\partial \bar{x}} + \bar{v}\frac{\partial}{\partial \bar{y}}\right)\bar{T} = k_{nf}\left(\frac{\partial^2 \bar{T}}{\partial \bar{x}^2} + \frac{\partial^2\, \bar{T}}{\partial \bar{y}^2}\right) + \mu_{nf}(4\left(\frac{\partial \bar{u}}{\partial \bar{x}}\right)^2 + (\frac{\partial \bar{v}}{\partial \bar{x}} + \frac{\partial \bar{u}}{\partial \bar{y}})^2 - \frac{\partial q_r}{\partial \bar{y}} + Q_0 \tag{15}$$

Using the non-dimensional quantities listed below:

$x = \frac{\bar{x}}{\lambda}$	$y = \frac{\bar{y}}{d_1}$	$p = \frac{d_1^2 \bar{p}}{C\lambda\mu_f}$	$H_y = \frac{\bar{H}_y}{H_0}$
$u = \frac{\bar{u}}{C}$	$v = \frac{\bar{v}}{C}$	$R_e = \frac{\rho_f C d_1}{\mu_f}$	$H_x = \frac{\bar{H}_x}{H_0}$
$\delta = \frac{d_1}{\lambda}$	$E = -\frac{\bar{E}}{C H_0 \mu_e}$	$R_m = \sigma_f \mu_e C d_1$	$\theta = \frac{T - T_u}{T_l - T_u}$
$t = C\frac{\bar{t}}{\lambda}$	$R_d = \frac{4\sigma_f^*(T_l - T_u)^3}{3k_f^* k_f}$	$S^2 = \frac{M^2}{R_e R_m}$	$P_r = \frac{\mu_f (c_p)_f}{k_f}$
$\phi = \frac{\bar{\phi}}{H_0 d_1}$	$\beta = \frac{Q_0 d_1^2}{k_f (T_l - T_u)}$	$M = H_0 d_1 \sqrt{\frac{\sigma_f}{\mu_f}}$	$E_c = \frac{C^2}{(c_p)_f (T_l - T_u)}$
$A_1 = \frac{\rho_{nf}}{\rho_f}$	$A_2 = \frac{\mu_{nf}}{\mu_f}$	$A_5 = \frac{(\rho c_p)_{nf}}{(\rho c_p)_f}$	$A_4 = \frac{k_{nf}}{k_f}$

In the preceding expressions T_u is temperature at upper wall , T_l is temperature at lower wall , $\bar{\psi}$ is stream function, E is strength of the electric field, δ is wavenumber, R_e *is* Reynolds number, Ω is rotation, R_m is magnetic Reynolds number, E_c isEckert number, P_r is Prandtl number, $\bar{\phi}$ *is* magnetic force function, M is Hartmann number, θ is temperature in the non-dimensional form , β is internal heat generation, and S is Strommer number respectively, the non-dimensional form of the peristaltic wave can be expressed by :

$h = \frac{\bar{h}}{d_1} = 1 + \epsilon\, Sin\,(2\pi x)$, where amplitude ratio $\epsilon = \frac{d_2}{d_1}$.

Introduction of dimensionless magnetic force function ϕ and stream function ψ by using the relations :

$$u = \frac{\partial \psi}{\partial y}\,, v = -\delta\frac{\partial \psi}{\partial x}\,,\; H_x = \frac{\partial \varphi}{\partial y} \quad ,\; H_y = -\delta\frac{\partial \varphi}{\partial x} \tag{16}$$

Substituting Eq.(16) into Eqs. (12 -15), giving us the equations:

$$A_1 Re\,\delta\left(\psi_y\frac{\partial}{\partial x} - \psi_x\frac{\partial}{\partial y}\right)\psi_y - \frac{\rho_{nf}\,d_1^2}{\mu_f}\Omega^2(\psi_y) = -(P_m)_x + A_2\nabla^2\psi_y + S^2 Re\big(\delta\phi_y\phi_{xy} - \delta\phi_x\phi_{yy} + \phi_{yy}\big) \tag{17}$$

$$A_1 Re\delta^3\left(\psi_y\frac{\partial}{\partial x} - \psi_x\frac{\partial}{\partial y}\right)\psi_x - \frac{\rho_{nf}\,d_1^2}{\mu_f}\Omega^2\delta^2\psi_x = (P_m)_y + A_2\,\delta^2\nabla^2\psi_x + S^2 Re\delta^2\big(\delta\phi_y\phi_{xx} - \delta\phi_x\phi_{xy} + \phi_{xy}\big) \tag{18}$$

$$E = (\psi_y - \delta\big(\psi_y\phi_x - \psi_x\phi_y\big) + \frac{1}{A_3 R_m.}\nabla^2\phi \tag{19}$$

$$A_5 Re\ P_r \delta\left(\psi_y \theta_x - \psi_x \theta_y\right) = A_4 \nabla^2 \theta + A_2\ E_c\ P_r \left(4\delta^2 \psi_{xy}^2 + \left(\psi_{yy} - \delta^2 \psi_{xx}\right)^2\right) + R_d (\theta^4)_{yy} + \beta \qquad (20)$$

$Where\ P_m$ is the sum magnetic and ordinary pressure, which is the total pressure. The corresponding stream function, temperature function, and magnetic force function boundaries for non-conductive elastic walls in the wave frame are as follows:

$$\psi = 0,\quad \phi_y = 0,\ \psi_{yy} = 0, at\quad y = 0,$$
$$\phi = 0, \psi_y = -1, \theta = 0, \psi = \frac{q}{2}, at\quad y = h,$$
$$\theta = 1 \quad at \quad y = -h\,. \qquad (21)$$

Where q represent mean of flow rate. Using the long wave length approximation and neglect the wavenumber along the low Reynolds number, one can find from Equations (17)- (20) That:

$$(P_m)_x = \frac{\rho_{nf}\, d_1^2}{\mu_f} \Omega^2 \psi_y + A_2 \psi_{yyy} + S^2 Re \phi_{yy} \qquad (22)$$

$$(P_m)_y = 0 \qquad (23)$$

$$E = \psi_y + \frac{1}{A_3 R_m.} \phi_{yy} \qquad (24)$$

$$\theta_{yy} = \frac{1}{A_4}\left(-A_2\ E_c\ P_r \left(\psi_{yy}\right)^2 - R_d (\theta^4)_{yy} - \beta\ \right) \qquad (25)$$

By using cross derivation to eliminate the pressure from Eq.(22) and Eq.(23), giving us the equation:

$$\frac{\rho_{nf}\, d_1^2}{\mu_f} \Omega^2 \psi_{yy} + A_2 \psi_{yyyy} + S^2 Re \phi_{yyy} = 0 \qquad (26)$$

Join Eq.s (24) and (26), become :

$$\psi_{yyyy} = \frac{-1}{A_2} (M^2 A_3 \psi_{yy} + K \psi_{yy}) \qquad (27)$$

Where $K = \frac{\rho_{nf}\, d_1^2}{\mu_f} \Omega^2$.

4. Solution of the Problem

In this section, the Adomain decomposition method solution will be determined for the stream function, temperature, and magnetic force equation. In the operator $L_{iy}(*) = \frac{\partial^m (*)}{\partial y^m}$ apply Eqs. (27,24,and 25) in accordance with the Adomain decomposition method:

$$L_{yyyy} \psi = \frac{-1}{A_2} (M^2 A_3 \psi_{yy} + K \psi_{yy}) \qquad (28)$$

$$L_{yy} \phi = E A_3 R_m - \psi_y \qquad (29)$$

$$L_{yy}\theta = \frac{1}{A_4}\left(-A_2\, E_c\;\; P_r\left(\psi_{yy}\right)^2 - R_d(\theta^4)_{yy} - \beta\right) \tag{30}$$

Applying the inverse operator $L_{iy}^{-1}(*) = \underbrace{\int_0^y (*)dy}_{m-times}, i = 1,2,3, \ldots$,allows us to write Eqs(28-30):

$$\psi = L_{yyyy}^{-1}\left(\frac{-1}{A_2}(M^2 A_3\psi_{yy} + K\psi_{yy})\right) \tag{31}$$

$$\phi = L_{yy}^{-1}(EA_3R_m - \psi_y) \tag{32}$$

$$\theta = L_{yy}^{-1}\left(\frac{1}{A_4}\left(-A_2\, E_c\;\; P_r\left(\psi_{yy}\right)^2 - R_d(\theta^4)_{yy} - \beta\right)\right. \tag{33}$$

Decompose the stream function, temperature, and magnetic force equations using boundary equation (21).

$$\psi = \sum_{m=0}^{\infty} \psi_m,\ \phi = \sum_{m=0}^{\infty} \phi_m,\quad \theta = \sum_{m=0}^{\infty} \theta_m \tag{34}$$

By definition of L_{iy}^{-1},giving us

$$\psi_0 = \frac{1}{2}y^2C_1 + \frac{1}{6}y^3C_2 + C_3 + yC_4$$

$$\phi_0 = -\frac{A_3}{2}\mathrm{ERm} + \frac{A_3}{2}E\mathrm{Rm}y^2$$

$$\theta_0 = -\frac{-h^2\beta - A_4}{2A_4} + y\left(-\frac{1}{2h}\right) - \frac{y^2\beta}{2A_4} \tag{35}$$

$$\psi_{n+1} = L_{yyyy}^{-1}\left(\frac{-1}{A_2}(M^2A_3\psi_{nyy} + K\psi_{nyy})\right)$$

$$\phi_{n+1} = L_{yy}^{-1}(\psi_{ny})$$

$$\theta_{n+1} = L_{yy}^{-1}\left(\frac{1}{A_4}\left(-A_2\, E_c\;\; P_r\left(\psi_{nyy}\right)^2 - R_d(\theta_n^4)_{yy}\right)\right. \tag{36}$$

Due to length colocation ,they have computed up to the second term only :

$$\psi_1 = C_5 + yC_6 + y^2C_7 + y^3C_8 + \frac{Ky^5}{40h^2A_2} + \frac{Kqy^5}{80h^3A_2} - \frac{M^2y^5A_3}{40h^2A_2} - \frac{M^2qy^5A_3}{80h^3A_2},$$

$$\phi_1 = s_1 + ys_2 + \frac{\mathrm{Rm}(-\frac{1}{2}h^2(2h+3q)y^2 + \frac{1}{4}(2h+q)y^4)A_3}{4h^3},$$

$$\theta_1 = c_1 + yc_2 - \frac{1}{16h^6A_4^5}y^2\big(h^6\mathrm{Rd}(-4h^6+6h^4y^2-4h^2y^4+y^6)\beta^4 - 4h^5\mathrm{Rd}(3h^5-3h^4y-3h^3y^2+3h^2y^3+hy^4-y^5)\beta^3A_4 - 6h^4\mathrm{Rd}(h^4-4h^3y+h^2y^2+2hy^3-y^4)\beta^2A_4^2 + 4h^3\mathrm{Rd}(2h^3+2h^2y-3hy^2+y^3)\beta A_4^3 + A_4^4(h^2\mathrm{Rd}(6h^2-4hy+y^2)+3\mathrm{Ec}(2h+q)^2y^2A_2p_r)\big),$$

$$\psi_2 = C_9 + yC_{10} + y^2C_{11} + y^3C_{12} - \frac{(2h+q)(K-M^2A_3)\left(-6y^5A_2+\frac{1}{35}y^5(-21h^2+5y^2)(K-M^2A_3)\right)}{480h^3A_2^2},$$

$$\phi_2 = s_3 + ys_4 + \frac{\mathrm{Rm}A_3(-10h^2(2h+3q)y^2A_2+5(2h+q)y^4A_2+\frac{1}{6}(2h+q)(h^2-y^2)^3(K-M^2A_3))}{80h^3A_2},$$

$$\theta_2 = c_3 + yc_4 - \frac{1}{102400h^{24}A_2A_4^{21}}(c_5 - 25h^{54}\mathrm{Rd}^5y^2\beta^{16}A_2 + \frac{375}{2}h^{52}\mathrm{Rd}^5y^4\beta^{16}A_2 - 875h^{50}\mathrm{Rd}^5y^6\beta^{16}A_2 + \frac{11375}{4}h^{48}\mathrm{Rd}^5y^8\beta^{16}A_2 - 6825h^{46}\mathrm{Rd}^5y^{10}\beta^{16}A_2 + \frac{25025}{2}h^{44}\mathrm{Rd}^5y^{12}\beta^{16}A_2 - 17875h^{42}\mathrm{Rd}^5y^{14}\beta^{16}A_2 + \frac{160875}{8}h^{40}\mathrm{Rd}^5y^{16}\beta^{16}A_2 - 17875h^{38}\mathrm{Rd}^5y^{18}\beta^{16}A_2 + \frac{25025}{2}h^{36}\mathrm{Rd}^5y^{20}\beta^{16}A_2 - 6825h^{34}\mathrm{Rd}^5y^{22}\beta^{16}A_2 + \frac{11375}{4}h^{32}\mathrm{Rd}^5y^{24}\beta^{16}A_2 - 875h^{30}\mathrm{Rd}^5y^{26}\beta^{16}A_2 + \frac{375}{2}h^{28}\mathrm{Rd}^5y^{28}\beta^{16}A_2$$

$$-25h^{26}\mathrm{Rd}^5y^{30}\beta^{16}A_2 + \frac{25}{16}h^{24}\mathrm{Rd}^5y^{32}\beta^{16}A_2 - 375h^{52}\mathrm{Rd}^5y^2\beta^{15}A_2A_4 + 375h^{51}\mathrm{Rd}^5y^3\beta^{15}A_2A_4 + 2625h^{50}\mathrm{Rd}^5y^4\beta^{15}A_2A_4 - 2625h^{49}\mathrm{Rd}^5y^5\beta^{15}A_2A_4 - 11375h^{48}\mathrm{Rd}^5y^6\beta^{15}A_2A_4 + 11375h^{47}\mathrm{Rd}^5y^7\beta^{15}A_2A_4 + 34125h^{46}\mathrm{Rd}^5y^8\beta^{15}A_2A_4 - 34125h^{45}\mathrm{Rd}^5y^9\beta^{15}A_2A_4 - 75075h^{44}\mathrm{Rd}^5y^{10}\beta^{15}A_2A_4 + 75075h^{43}\mathrm{Rd}^5y^{11}\beta^{15}A_2A_4 + 125125h^{42}\mathrm{Rd}^5y^{12}\beta^{15}A_2A_4 - 125125h^{41}\mathrm{Rd}^5y^{13}\beta^{15}A_2A_4 - 160875h^{40}\mathrm{Rd}^5y^{14}\beta^{15}A_2A_4 + 160875h^{39}\mathrm{Rd}^5y^{15}\beta^{15}A_2A_4).$$

The $c_1,\ldots, c_5$, $C_1, \ldots, C_{12}$, and $s_1,..,s_4$ are large constants coefficients can be determined by using boundary condition Eq.(21) and MATHMATICA software. So on. Then the approximation system solution takes the following form:

$$\psi = \psi_0 + \psi_1 + \psi_2 + \cdots,$$

$$\phi = \phi_0 + \phi_1 + \phi_2 + \cdots,$$

$\theta = \theta_0 + \theta_1 + \theta_2 + \cdots.$

The equation for the coefficient of heat transfer at the wall is:

$$Z = \xi_x \theta_y \tag{37}$$

So,the electric field E is obtain from :

$$E = \psi_y + \frac{1}{A_3 R_m.} \phi_{yy} .$$

5. Discussion and Graphs of the Results

The purpose of this section is to examine the graphic results of a variety of important parameter utilized in the specified modeling. In particular, streamlines, velocity, induced magnetic field, magnetic force contours, heat transfer coefficient, and temperature distribution are depicted in the figures below. We examined numerous cases, including the Hartmann number M, the magnetic Reynolds number Rm,and rotation Ω. The numerical variables were chosen based on previous literature[26-28], and flow trapping is discussed graphically. All figures are plotted using from the MATHEMATICA program.

5.1 Velocity Profile

Figure1 depicts the velocity changes with respect to the axial y for various Hartmann number M, rotation, and dynamic viscosity values μ. The effect of Hartmann number M on velocity is shown in Fig.1a. As M increases, the velocity u near the channel's middle rises, whereas the opposite occurs near the peristaltic wall. This fact is related to the Lorentz force, which occurs when an external magnetic field is used and, in turn, leads the fluid motion to slow down. It demonstrates that the Lorentz force is much stronger near the wall than in the channel's middle. Display the effect of dynamic viscosity on velocity in Fig.1b. It is noticed that when μ increases, the velocity along the channel walls slowly decreases, whereas it increases at the channel center. Fig.1c displays the rotational effect. It can be seen that as rotation increases, the velocity u decreases near the channel's middle, whereas the reverse behavior can be seen near the peristaltic wall.

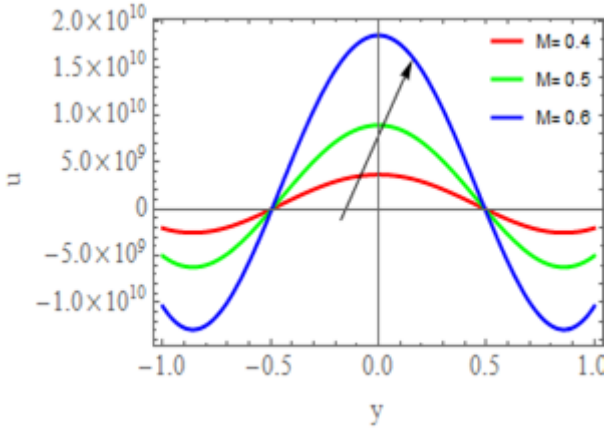

Figure1a. Impact of M on the velocity u

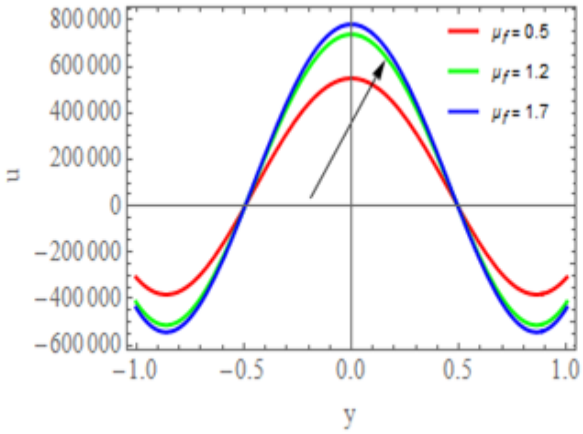

Figure 1b. Impact of μ on the velocity u

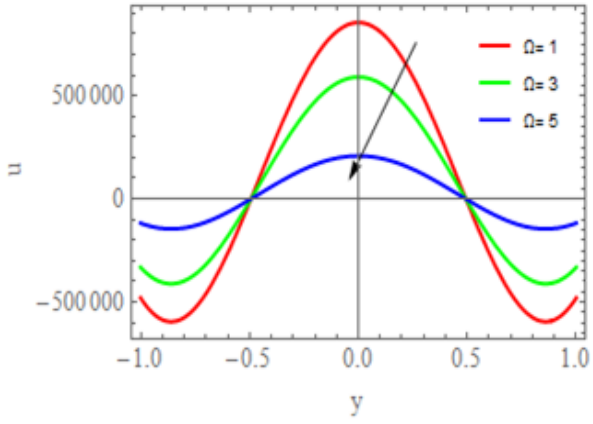

Figure 1c. Impact of Ω on the velocity u

5.2 Induced Magnetic Field Profile

This subsection describes an examination of induced magnetic field H_x. Graphics have been drawn to show the development of the induced magnetic field profile in Figure 2.

To study the impacts of magnetic Reynolds numbers Rm, Hartmann number M, and rotation Ω on the induced magnetic field H_x with respect to axial y. We are carried out from Figure 2a-2d.The effects of magnetic Reynolds number Rm, and magnetic field M on the induced magnetic field profile can be observed in Figs.2a and 2b. It is noticed that the relationship between H_x and y is inversely proportional to each other , with the rise in Rm and M in the region $y \leq 0$,the induced magnetic field decreases and while in the region $y \geq 0$, the induced magnetic field H_x rises with the increase in Rm and M. The impact of rotation Ω on the induced magnetic field H_x is seen in Fig.2c. At $y \geq 0$, the induced magnetic field H_x increases as rotation Ω increases, but it decreases at $y \leq 0$.

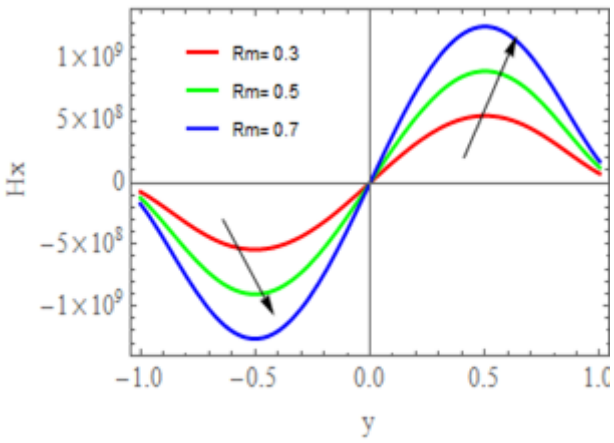

Figure 2a. Impact of Rm on the induced magnetic field profile

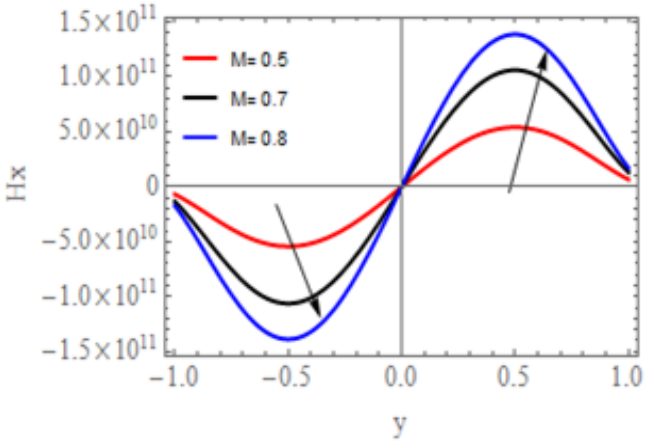

Figure 2b. Impact of M on the induced magnetic field profile

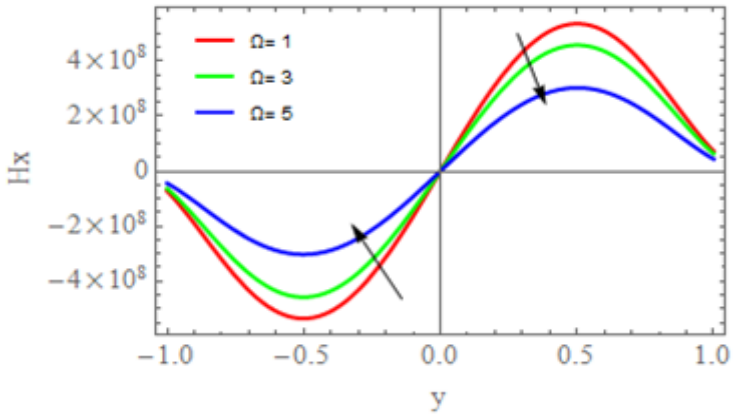

Figure 2c. Impact of M on the induced magnetic field profile

5.3 Temperature Profile

The temperature profile behavior for the Hartmann number M, heat radiation Rd, rotation Ω, heat absorption β, Eckert number Ec, and Prandtl number pr are examined in Figure3.

The impact of Hartmann number M on the temperature profile θ are examined by Fig.3a. If a rise in temperature is observed with increase values of Hartmann numbers M. The temperature profile θ enhances by increasing of Prandtl number Pr in Fig.3b, this is because heat generation form friction brought by shear in the flow is more pronounced when the fluid is highly viscous or moving quickly. Same behavior is observed for Eckert number that can be shown from Fig.3c As the rotation parameter values increase, the temperature profile is seen to decrease Fig. 3d.

Influence of heat absorption β is depicted in Fig. 3e the temperature profile θ decreases in the center of the channel and merges for near the wall.Fig.3f shows the impact of the radiation Rd on the temperature profile θ, initially, the θ decreases and then merges near the wall.

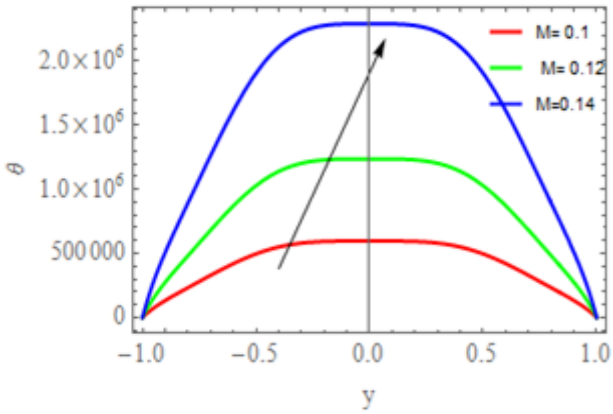

Figure 3a. Impact of M on the temperature profile

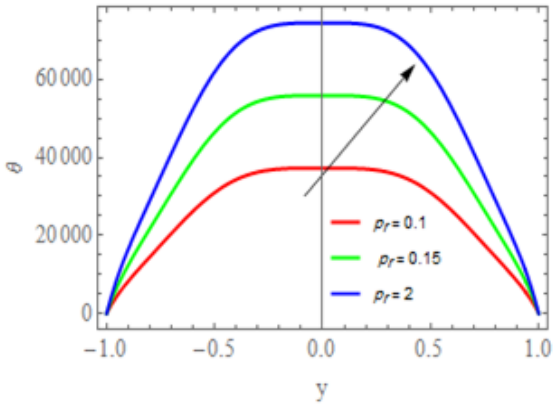

Figure 3b. Impact of Pr on the temperature profile

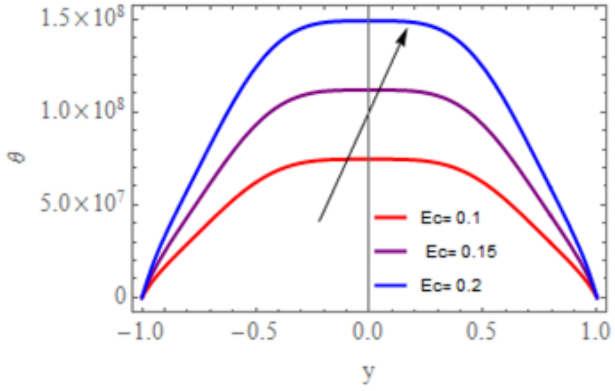

Figure 3c. Impact of Ec on the temperature profile

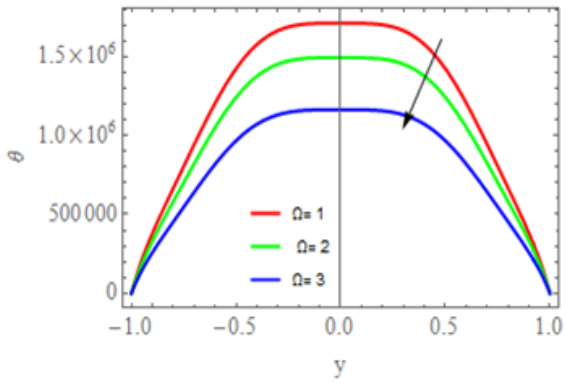

Figure 3d. Impact of Ω on the temperature profile

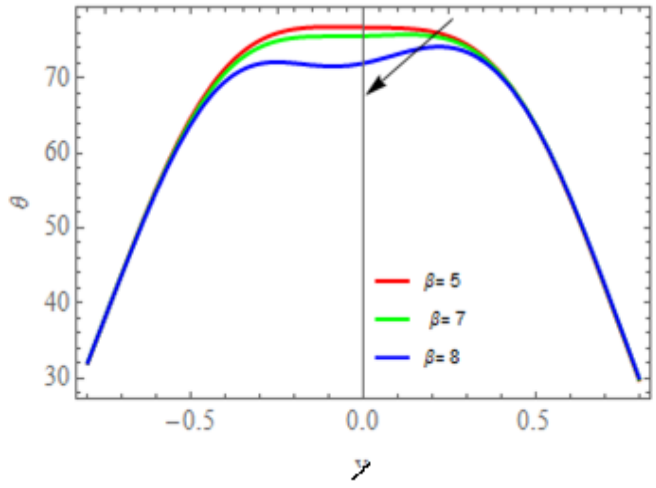

Figure 3d. Impact of β on the temperature profile

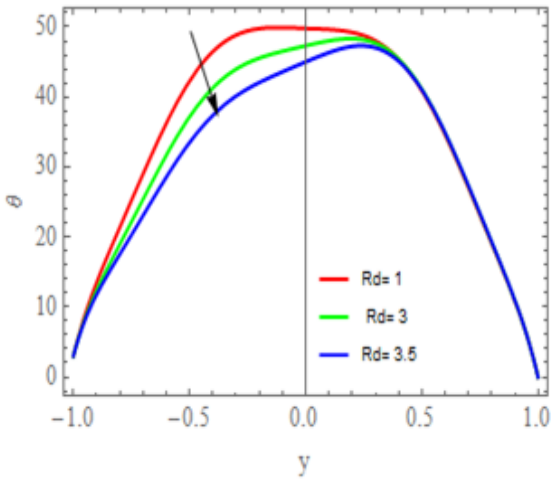

Figure 3e. Impact of Rd on the temperature profile

5.4 Heat Transfer Coefficient

The behaviors of Prandtl number p_r, heat absorption β, Eckert number E_c, rotation **Ω**, and heat radiation Rd on heat transfer coefficient Z have been noticed through Fig.4.

Fig.4a shows that when rotation increases, the heat transfer coefficient Z between the fluid and the wall of the channel decreases. In Fig.4b depicts the behavior of the heat transfer coefficient for various values of heat radiation Rd. An increase in the heat transfer is observed for rising values of the heat radiation Rd. The impact of Eckert number Ec and Prandtl number Pr on heat transfer coefficient, it is noticed from Fig.4c and 4d that heat transfer coefficient enhances for higher values of E_c and P_r.

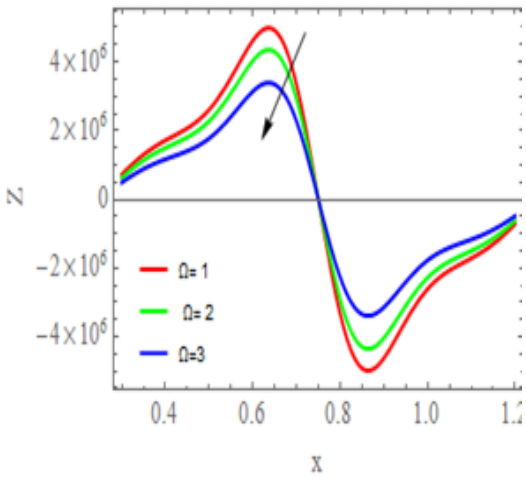

Figure 4a. Impact of Ω on the heat transfer coefficient

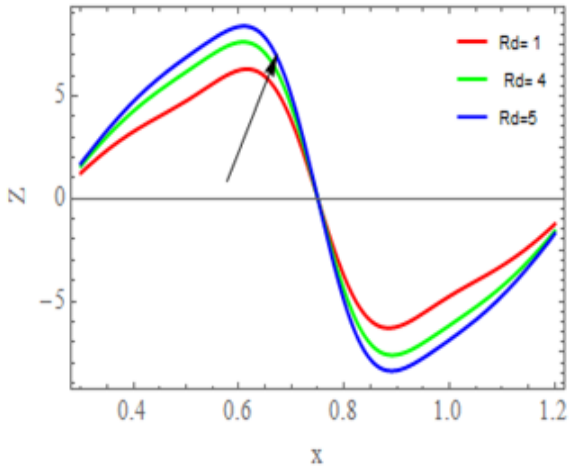

Figure 4b. Impact of Rd on the heat transfer coefficient

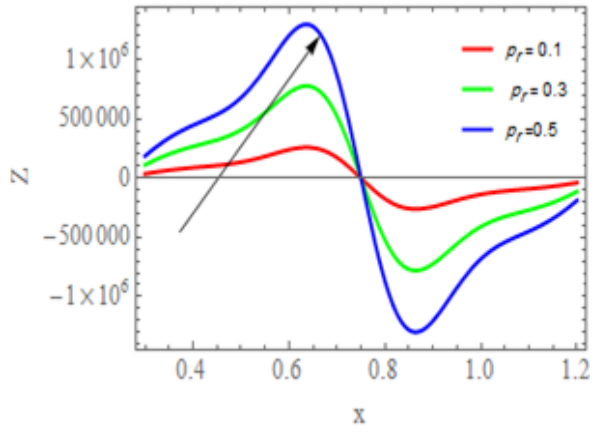

Figure 4c. Impact of pr on the heat transfer coefficient

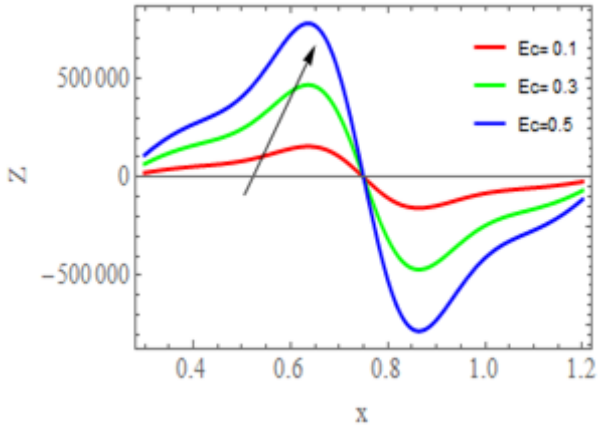

Figure 4d. Impact of Ec on the heat transfer coefficient

5.5 Trapping Phenomenon

Typically, streamlines have the same shape as a boundary wall in the wave frame. However, under certain situations, some stream lines split and enclose a bolus, which moves as a whole with the waves. "Trapping" is the term for this phenomenon. In order to investigate the impacts of the trapping phenomenon at various values of Hartmann number M and rotation Figs.5 and 6 were drawn. It can be shown from Fig.5 that as Hartmann number M increases, the trapped bolus rises in size. The impact of rotation Ω on trapping can be noticed from Fig .6, it is shown that when the value of Ω increases, the size of the trapped bolus diminishes.

Figs.7,8,and 9 show the magnetic force for various values of essential parameters. The contours of magnetic force are parallelly to the flow field. Fig.7 illustrates that rotation affects the magnetic force contours; it is observed that as rotation increases, the magnetic force lines diminish and the size of the bolus changes. Figs.8 and 9 illustrate how magnetic Reynolds number Rm and Hartmann number M influence the magnetic force contours. As the values of M and Rm are raised,the magnetic force contours move themselves forward and the magnetic force gradually increases, as can be seen in these figures.

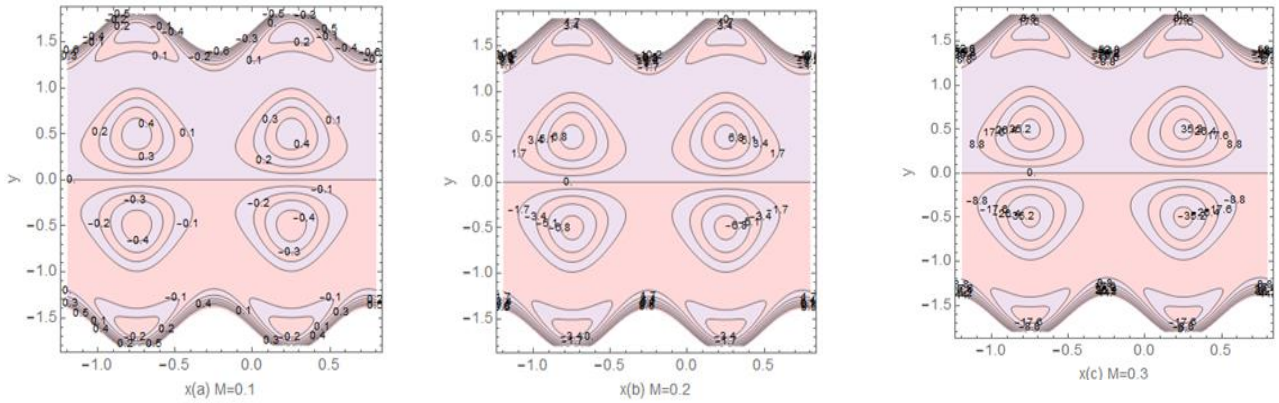

Figure 5. Impact of Hartmann number on the stream lines

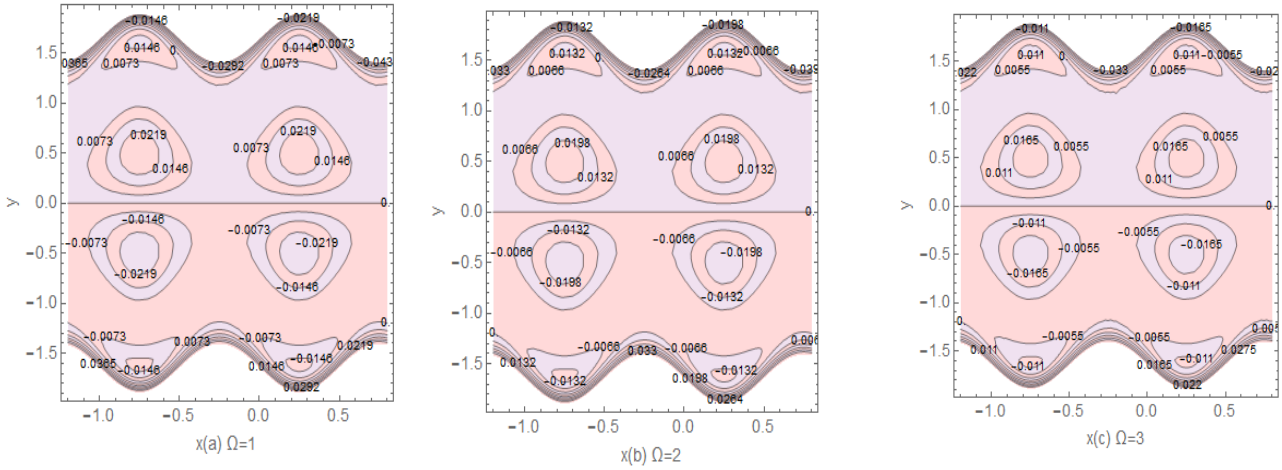

Figure 6. Impact of rotation on the stream lines

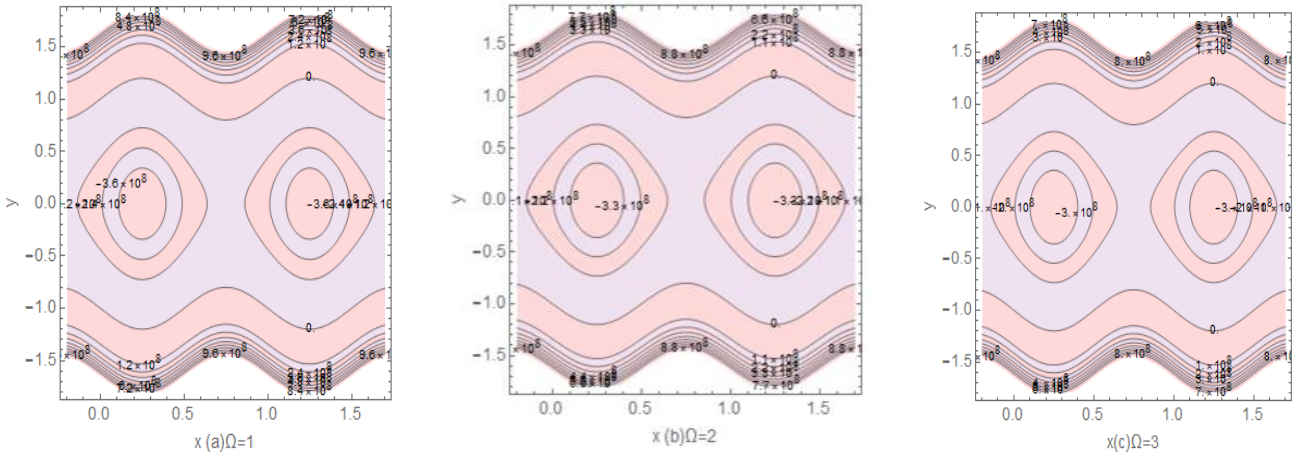

Figure 7. Impact of rotation on the magnetic force contours

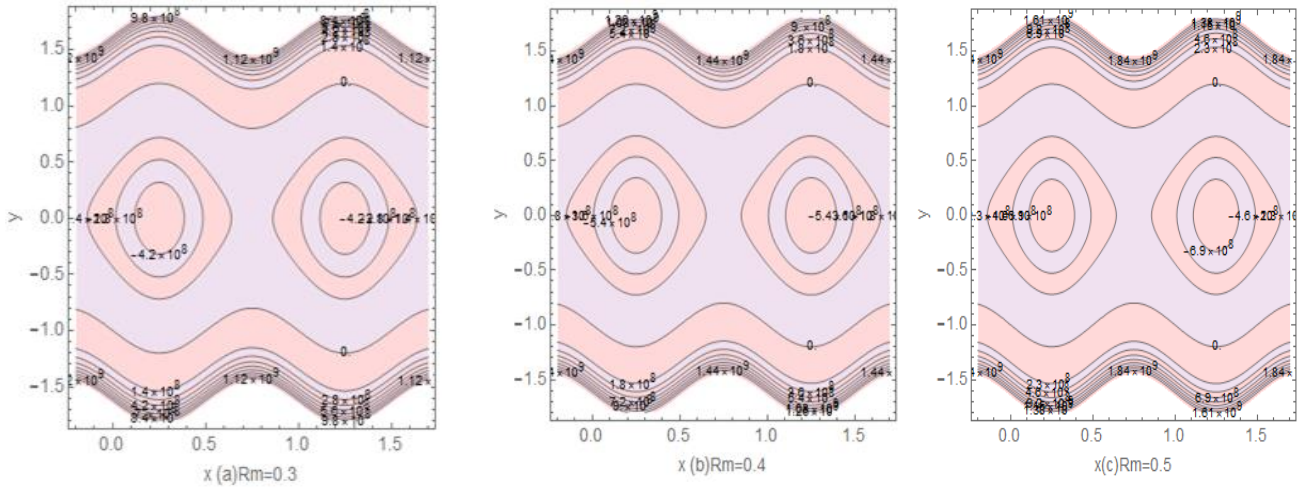

Figure 8. Impact of Reynolds number on the magnetic force contours

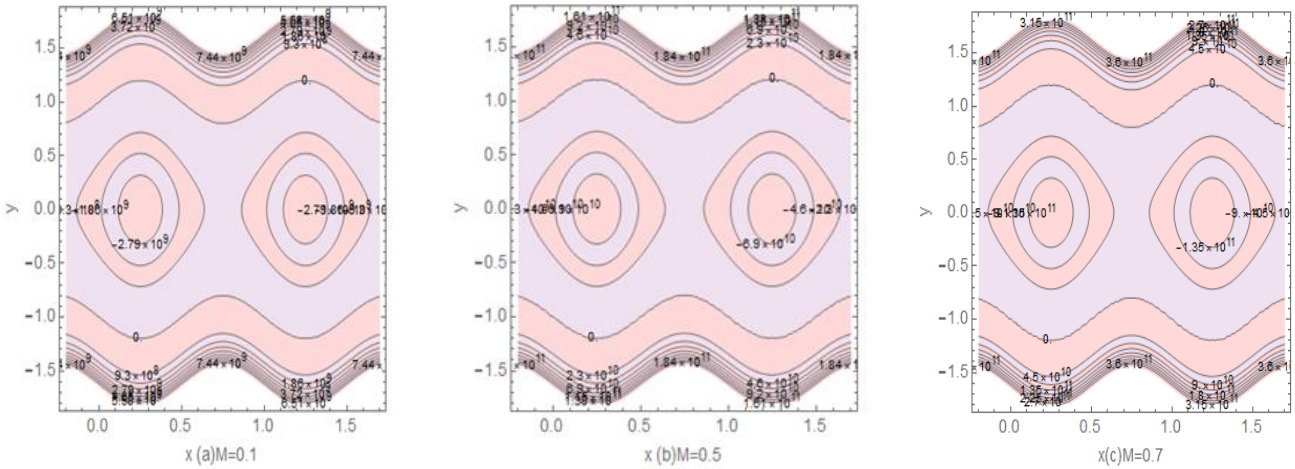

Figure 9. Impact of Hartmann number on the magnetic force contours

6. Conclusion

The impact of magnetic force ,rotation,and nonlinear heat radiation on hybrid bio-nanofluids peristaltic flow in a symmetric channel under the influence of a magnetic field are discussed. The governing equations representing momentum, Maxwell, and heat equations are considered. The exact expressions for velocity, heat transfer coefficient, stream lines, temperature, induced magnetic field, and magnetic force are obtained by using the Adomain decomposition method. The major results can be summarized as follows:

- The behavior of the velocity distribution u near the center part of the channel increases with a rises in Hartmann number M, while rotation parameters oppose the velocity.
- Induced magnetic field exhibits dual conduct in the two zones $y \leq 0$, $y \geq 0$ against all the important parameters.
- The temperature profile in the Prandtl number Pr and the Eckert number Ec is improved.
- The temperature profile decline when higher values of rotation.
- The heat transfer coefficient raises with rising values of the radiation parameter, Prandtl number, and Hartmann number M, and decreases with rotation.

- The trapped bolus rises in size at increasing of Hartmann number M and decline at increasing of rotation.
- The contours of magnetic force improve because of an increase in the magnitude of Hartmann number M.
- The contours of magnetic force decrease because of an increase in the magnitude of the rotation Ω.

Finally, we conclude that the findings of this paper should be beneficial for researchers aiming to develop fluid mechanics as well as those in biomedical engineering and technology.

References

1. Zaman, A.; Ali, N.; Khan, A. A., Computational biomedical simulations of hybrid nanoparticles on unsteady blood hemodynamics in a stenotic artery. *Mathematics and Computers in Simulation,* **2020,** *169*, 117-132.
2. Changdar, S.; De, S. Investigation of nanoparticle as a drug carrier suspended in a blood flowing through an inclined multiple stenosed artery. *Bionanoscience* **2018,** *8* (1), 166-178.
3. Chen, P. C.; Mwakwari, S. C.; Oyelere, A. K. Gold nanoparticles: from nanomedicine to nanosensing. *Nanotechnology, science and applications***, 2008,** *1*, 45.
4. Hummady, L. Z.; Abbas, I. T.; Mohammed, R. A. Inclined Magnetic Field of Non-uniform and Porous Medium Channel on Couple Stress Peristaltic Flow and application in medical treatment (Knee Arthritis). *Journal of Southwest Jiaotong University,* **2019,** *54* (4).
5. Das, S.; Barman, B.; Jana, R. Influence of Hall and Ion-Slip Currents on Peristaltic Transport of Magneto-Nanofluid in an Asymmetric Channel. *BioNanoScience,* **2021,** *11* (3), 720-738.
6. Zhang, L.; Bhatti, M. M.; Marin, M.; S. Mekheimer, K. Entropy analysis on the blood flow through anisotropically tapered arteries filled with magnetic zinc-oxide (ZnO) nanoparticles. *Entropy,* **2020,** *22* (10), 1070.
7. Abbasi, F.; Gul, M.; Shehzad, S. Effectiveness of temperature-dependent properties of Au, Ag, Fe3O4, Cu nanoparticles in peristalsis of nanofluids. *International Communications in Heat and Mass Transfer,* **2020,** *116*, 104651.
8. Abo-Elkhair, R.; Bhatti, M.; Mekheimer, K. S. Magnetic force effects on peristaltic transport of hybrid bio-nanofluid (AuCu nanoparticles) with moderate Reynolds number: An expanding horizon. *International Communications in Heat and Mass Transfer,* **2021,** *123*, 105228.
9. Noreen, S.; Rashidi, M.; Qasim, M. Blood flow analysis with considering nanofluid effects in vertical channel. *Applied Nanoscience,* **2017,** *7* (5), 193-199.
10. Tripathi, D.; Prakash, J.; Gnaneswara Reddy, M.; Kumar, R. Numerical study of electroosmosis-induced alterations in peristaltic pumping of couple stress hybrid nanofluids through microchannel. *Indian Journal of Physics,* **2021,** *95 (11)*, 2411-2421.
11. Abd-Alla, A.; Mohamed, R.; Abo-Dahab, S.; Soliman, M. Rotation and initial stress effect on MHD peristaltic flow of reacting radiating fourth-grade nanofluid with viscous dissipation and Joule heating. *Waves in Random and Complex Media,* **2022**, 1-35.
12. Abd-Alla, A.; Abo-Dahab, S.; El-Shahrany, H. Effects of rotation and initial stress on peristaltic transport of fourth grade fluid with heat transfer and induced magnetic field. *Journal of Magnetism and Magnetic Materials,* **2014,** *349*, 268-280.
13. Salih, A. W. Influence Of Rotation, Variable Viscosity And Temperature On Peristaltic Transport In An Asymmetric Channel. *Turkish Journal of Computer and Mathematics Education ,* **2021,** *12* (6), 1047-1059.
14. Mohaisen, H. N.; Abedulhadi, A. M. Effects of the Rotation on the Mixed Convection Heat Transfer Analysis for the Peristaltic Transport of Viscoplastic Fluid in Asymmetric Channel. *Iraqi Journal of Science,* **2022**, 1240-1257.

15. Mohaisen, H. N.; Abdalhadi, A. M. Influence of the Induced Magnetic and Rotation on Mixed Convection Heat Transfer for the Peristaltic Transport of Bingham plastic Fluid in an Asymmetric Channel. *Iraqi Journal of Science*, **2022**, 1770-1785.
16. M. Abdulhadi, A.; Al-Hadad, A. H. Effects of rotation and MHD on the Nonlinear Peristaltic Flow of a Jeffery Fluid in an Asymmetric Channel through a Porous Medium. *Iraqi Journal of Science*, **2023,** *57* (1A), 223-240.
17. Hayat, T.; Rafiq, M.; Ahmad, B. Influences of rotation and thermophoresis on MHD peristaltic transport of Jeffrey fluid with convective conditions and wall properties. *Journal of Magnetism and Magnetic Materials*, **2016,** *410*, 89-99.
18. Mjthap, H. Z.; Al-Azzawi, S. N. Mixing Sumudu transform and Adomain decomposition method for solving Riccati equation of variable fractional order. *Journal of Interdisciplinary Mathematics*, **2019,** *22* (8), 1559-1563.
19. Tawfiq, L. N.; Hussein, N. A. Efficient Approach for Solving (2+ 1) D-Differential Equations. *Baghdad Science Journal*, **2022**, 0166-0166.
20. Wazwaz, A.-M., Adomian decomposition method for a reliable treatment of the Bratu-type equations. *Applied Mathematics and Computation,* **2005,** *166* (3), 652-663.
21. Bhatti, S.; Zahid, M.; Ali, R.; Sarwar, A.; Wahab, H. A. Blade coating analysis of a viscoelastic Carreau fluid using Adomian decomposition method. *Mathematics and Computers in Simulation,* **2021,** *190*, 659-677.
22. Shit, G.;Ranjit, N.; Sinha, A. Adomian decomposition method for magnetohydrodynamic flow of blood induced by peristaltic waves. *Journal of Mechanics in Medicine and Biology,* **2017,** *17* (01), 1750007.
23. Kareem, Z. H.; Tawfiq, L. N. M. Recent Modification of Decomposition Method for Solving Nonlinear Partial Differential Equations. *Journal of Advances in mathematics,* **2020,** *18*, 154-161.
24. Seikh, A. H.; Akinshilo, A.; Taheri, M.; Rahimi-Gorji, M.; Alharthi, N.; Khan, I.; Khan, A. R. Influence of the nanoparticles and uniform magnetic field on the slip blood flows in arterial vessels. *Physica Scripta,* **2019,** *94* (12), 125218.
25. Akram, J.; Akbar, N. S.; Tripathi, D. Blood-based graphene oxide nanofluid flow through capillary in the presence of electromagnetic fields: A Sutterby fluid model. *Microvascular Research* **2020,** *132*, 104062.
26. Raza, M.; Ellahi, R.; Sait, S. M.; Sarafraz, M.; Shadloo, M. S.; Waheed, I. Enhancement of heat transfer in peristaltic flow in a permeable channel under induced magnetic field using different CNTs. *Journal of Thermal Analysis and Calorimetry,* **2020,** *140* (3), 1277-1291.
27. Mekheimer, K. S.; Saleem, N.; Hayat, T.; Hendi, A. Simultaneous effects of induced magnetic field and heat and mass transfer on the peristaltic motion of second-order fluid in a channel. *International journal for numerical methods in fluids*, **2012,** *70* (3), 342-358.
28. Kareem, R. S.; Abdulhadi, A. M. Effect of MHD and Porous Media on Nanofluid Flow with Heat Transfer: Numerical Treatment. *Journal of advanced research in fluid mechanics and thermal science,* **2019,** *63* (2), 317-328.